Cent. Eur. J. Math. • 12(12) • 2014 • 1796-1810
DOI: 10.2478/s11533-014-0448-4

VERSITA

Central European Journal of **Mathematics**

Properties of triangulations obtained by the longest-edge bisection

Research Article

Francisco Perdomo[1*], Ángel Plaza[1†]

1 Division of Mathematics, Graphics and Computation (MAGiC), IUMA, Information and Communication Systems, and Department of Mathematics, University of Las Palmas de Gran Canaria, 35017 Las Palmas de Gran Canaria, Spain

Received 5 March 2013; accepted 26 January 2014

Abstract: The Longest-Edge (LE) bisection of a triangle is obtained by joining the midpoint of its longest edge with the opposite vertex. Here two properties of the longest-edge bisection scheme for triangles are proved. For any triangle, the number of distinct triangles (up to similarity) generated by longest-edge bisection is finite. In addition, if LE-bisection is iteratively applied to an initial triangle, then minimum angle of the resulting triangles is greater or equal than a half of the minimum angle of the initial angle. The novelty of the proofs is the use of an hyperbolic metric in a shape space for triangles.

MSC: 51M09, 65M50, 65N50

Keywords: Triangulation • Longest-edge bisection • Mesh refinement • Mesh regularity • Finite element method

1. Introduction

The finite element method requires *efficient* meshes (triangulations of surfaces) for the numerical algorithms to run. Although the requirements for meshes largely depend on the algorithm, the sharp (minimum/maximum) angle conditions seem to be a common feature of particular importance in this context [2, 6, 14]. For example, the longest-edge bisection algorithms guarantee the construction of high-quality triangulations [1, 11, 13, 24, 26, 27].

Regularity or non-degeneracy is one of the crucial properties required for simplicial meshes in finite element method. Several regularity criteria for triangular and tetrahedral finite element partitions have been proposed in literature [5, 16, 20]. Also, in several triangle partitions properties on mesh quality improvement have been studied [15, 21].

* *E-mail: kabayakawa@gmail.com*
† *E-mail: aplaza@dmat.ulpgc.es*

With respect to the longest-edge (LE) bisection of triangles the most classical result is due to Rosenberg and Stenger [24]. They showed the non-degeneracy property for LE-bisection by studying angles generated: if α_0 is the minimum angle of the given triangle, and α_n is the minimum interior angle among all new triangles produced at iteration n, then $\alpha_n \geq \alpha_0/2$.

Another important property of the longest-edge bisection of triangles is the finiteness of the number of triangles obtained up to similarity [1, 26, 27]. The main goal of this paper is to provide with new proofs for these two important properties of the longest-edge bisection for triangles. The proofs given here are new and use concepts from hyperbolic geometry in a space of normalized triangles. Hyperbolic geometry has been employed in other problems in computational geometry. See in this sense [3, 8, 9] and references therein. While previous demonstrations employed *ad hoc* methods of Euclidean geometry, the methodology of the proofs given here is generalizable to other partition methods [17–19]. The proofs are not necessarily shorter, but they are structured in an systematic way.

The structure of the paper is as follows. In Section 2, we introduce a scheme for normalizing triangles [10, 22]. In Section 3, we present the elements of hyperbolic geometry that will be used later. The result on the finiteness of the number of distinct (up to similarity) triangles generated is proved in Section 4. Section 5 is devoted to the new proof of the non–degeneracy property of the longest-edge bisection. Finally, a summarized version of some of the conclusions is given.

2. Triangle normalization

One of methods used in the literature on triangular mesh refinement is to normalize triangles [10, 17, 22]. The method consists of applying several possible isometries and dilations to a triangle, in such way one side can be identify with the segment whose endpoints are $(0,0)$ and $(1,0)$ with twelve posibilities, in general. See Figure 1. Leaving the free vertex in the upper half-plane, the longest-edge attached to the unitary segment and the shortest edge to the left, there are a single position for the free vertex. In this way, all similar triangles are characterized by a unique complex number z in the normalized region $\Sigma = \{0 < \mathrm{Re}(z) \leq 1/2,\ \mathrm{Im}(z) > 0, |z-1| \leq 1\}$. See Figure 2. Real and imaginary parts of complex number z are called Bookstein coordinates [4, 7].

Figure 1. A triangle with vertices z_1, z_2, z_3 can be attached to the segment $(0,0)$ and $(1,0)$ in twelve ways.

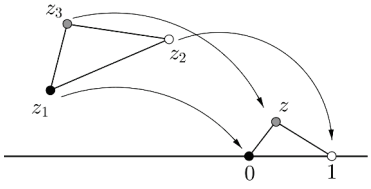

The LE-bisection of a triangle Δ is obtained by joining the midpoint on the longest edge of the triangle to the opposite vertex. Two new triangles are denoted as follows: the left triangle, Δ_L, and the right triangle, Δ_R.

The normalization of the left triangle Δ_L gives a complex number $w_L(z)$. In the same way the normalization of the right triangle Δ_R gives a complex number $w_R(z)$. Note that the normalization process depends on which edge in each sub-triangle is the longest one. Figure 3 shows how the normalization of the right triangle produced by the longest-edge bisection defines complex variable function $w_R(z)$ in that particular case. In the right triangle Δ_R, in grey in the figure, the longest edge is marked by *LE* and the opposite vertex is coloured. In this way, for an initial triangle with associated complex number z, we obtain two complex numbers $w_L(z)$ and $w_R(z)$, corresponding to the final position of the opposite vertex to the longest edge of each sub-triangle, after they have been normalized.

The normalization process of the left and right triangles generated by the LE-bisection depends on the lengths of the sides of the initial triangle and their relative positions. Therefore, for each one of the functions $w_L(z)$ and $w_R(z)$, there are subdomains in the normalized region where that function has the same expression. The expressions of the piecewise functions $w_L(z)$ and $w_R(z)$, are given in Figure 4, where also the boundaries between subdomains are provided.

Figure 2. The normalized region $\Sigma = \{0 < \mathrm{Re}(z) \leq 1/2,\ \mathrm{Im}(z) > 0, |z-1| \leq 1\}$.

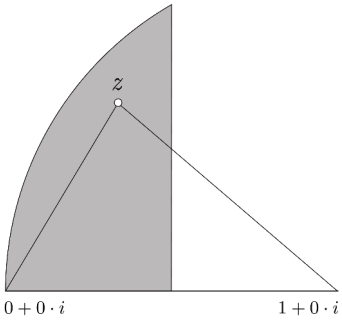

Figure 3. Example of geometric transformations to obtain function $w_R(z)$, where the longest-edge of the right triangle is as depicted in (a), and the second longest-edge of that triangle is of length $1/2$. In this case, $w_R(z) = \frac{2\bar{z}-1}{2\bar{z}-2}$.

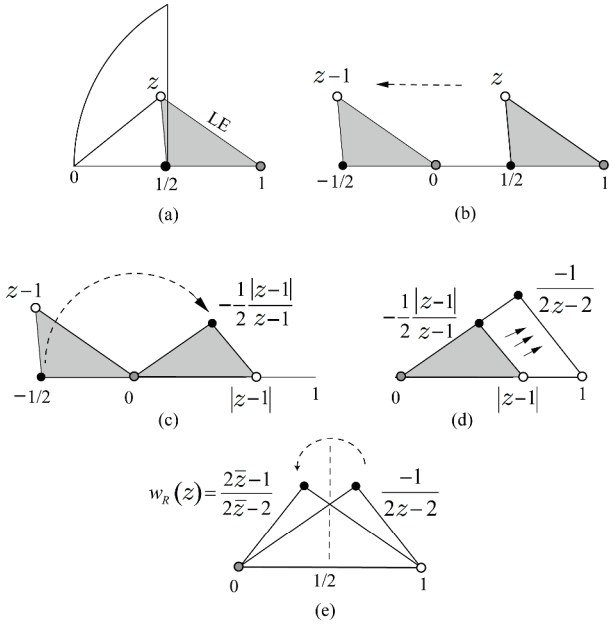

By way of example, we reproduce the derivation of function $w_R(z)$ for z with $|z-1/2| \leq 1/2$ in the normalized region. The second longest edge of the triangle with vertices $1/2$, 1, z is $[1/2,\ 1]$, while the shortest edge is $[1/2,\ z]$. See Figure 3. The longest edge of the right triangle (triangle in grey in Figure 3 (a)) joins point 1 to the affix of the complex number z. We translate the right triangle as in Figure 3 (b) and then the triangle is rotated so that the longest edge is over the real axis, see Figure 3 (c). Then the longest edge is normalized to 1 through a dilation of rate $\frac{1}{|z-1|}$, as depicted in Figure 3 (d). In the last step, Figure 3 (e), a reflection with respect to the line $\mathrm{Re}(z) = 1/2$ is applied to the complex $\frac{-1}{2z-2}$ for obtaining $w_R(z) = \frac{2\bar{z}-1}{2\bar{z}-2}$.

3. Hyperbolic distance

We use the results of hyperbolic geometry and particularly the Poincare half-plane model [12, 25, 28] in this paper.

Figure 4. Piecewise functions $w_L(z)$ (left), and $w_R(z)$ (right) depending on the position of point z.

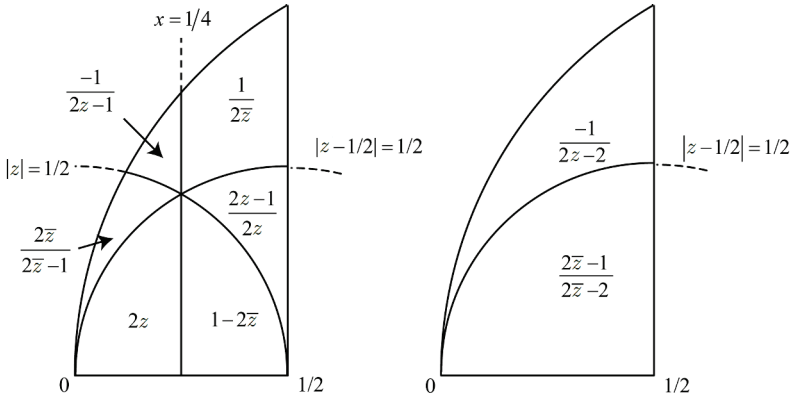

The circumferences and straight lines appearing in the definitions of piecewise functions w_L and w_R are orthogonal to the line $\operatorname{Im} z = 0$, and are geodesics in the Poincare half-plane. The expressions for functions w_L and w_R are isometries in the half-plane hyperbolic model since they have the form $\frac{az+b}{cz+d}$ or $\frac{a(-\bar{z})+b}{c(-\bar{z})+d}$ with real coefficients verifying $a\,d - b\,c > 0$.

The functions w_L and w_R are symmetric with respect to the circumferences and to the straight lines which appear on the boundary of two neighbouring zones of the normalized region.

Lemma 3.1.

Let W be any of the functions w_L and w_R. Then W is invariant under inversion with respect to the circumferences (or under symmetry with respect to the straight line) which appear in its definition.

Proof. It is enough to check that all the expression of functions W verify the property. For example, let $W = w_R$. The inversion with respect to $\left|z - \frac{1}{2}\right| = \frac{1}{2}$ is given by $z \mapsto \frac{\bar{z}}{2\bar{z}-1}$. Its composition with $\frac{2z-1}{2z-2}$ is $\frac{-1}{2z-2}$. Or another example, let $W = w_L$. The symmetry with respect to $\operatorname{Re} z = 1/4$ is given by $z \mapsto \frac{1}{2} - \bar{z}$. The composition of this symmetry with, for example, the expression $\frac{1}{2z}$ results in $\frac{-1}{2z-1}$. The other cases can be proven with similar considerations. □

Here, for convenience, we recall some results for hyperbolic distance. If z_1 and z_2 are complex numbers with $\operatorname{Im} z_1 > 0$ and $\operatorname{Im} z_2 > 0$, then the hyperbolic distance d between z_1 and z_2 is defined by the formula

$$\cosh\ d(z_1, z_2) = 1 + \frac{|z_1 - z_2|^2}{2\ \operatorname{Im} z_1\ \operatorname{Im} z_2}. \tag{1}$$

If z_1 and z_2 have the same real parts, then

$$d(z_1, z_2) = \left|\ln\left(\frac{\operatorname{Im} z_1}{\operatorname{Im} z_2}\right)\right|. \tag{2}$$

If z_1 and z_2 are points in a geodesic circumference, and z_2 is the top point directly over the centre of the circumference, the hyperbolic length of the segment in the geodesic from z_1 to z_2, say l, verifies

$$\theta = 2\arctan\left(e^{-l}\right) \tag{3}$$

where θ is the difference between $\pi/2$ and the central angle determined by the segment from z_1 to z_2 over the geodesic. See Figure 5.

The following property assures that functions w_L and w_R do not increase the distance between points in the normalized region of space of triangles.

Figure 5. Illustration for Equation (3).

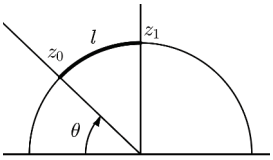

Lemma 3.2 (Non-increasing property).
Let W be any of the functions w_L and w_R. For any points z_1 and z_2 in the normalized region,

$$d(W(z_1), W(z_2)) \leq d(z_1, z_2) \tag{4}$$

where $d(\cdot,\cdot)$ denotes the hyperbolic distance on the half-plane.

Proof. If z_1 and z_2 are in a region with the same definition of W, then $d(z_1, z_2) = d(W(z_1), W(z_2))$, because W is an isometry on the half-plane hyperbolic model. Let us now suppose that z_1 and z_2 are not in a region with the same definition of W. We have two possibilities:

(1) z_1 and z_2 are in two regions with a common boundary. There exists z_1' in the region of z_2 with $W(z_1) = W(z_1')$ due to the symmetry of W with respect to the boundary. Let γ be the geodesic line that joins z_1 and z_2. γ intersects the boundary at a point, say z^*. Then $d(z_1, z_2) = d(z_1, z^*) + d(z^*, z_2)$ because the three points are in the same geodesic. $d(z_1, z^*) = d(z_1', z^*)$, since z_1 and z_1' are symmetrical points with respect to the boundary containing z^*. See Figure 6.

Figure 6. Illustration for Lemma 3.2: The geodesic line that joins z_1 and z^* is image by reflection of the segment joining z_1' with z^*, from where $d(z_1, z^*) = d(z_1', z^*)$.

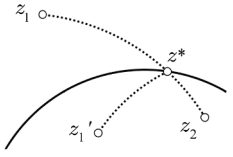

Therefore, by the triangular inequality,

$$d(z_1, z_2) = d(z_1, z^*) + d(z^*, z_2) = d(z_1', z^*) + d(z^*, z_2) > d(z_1', z_2).$$

Thus $d(W(z_1), W(z_2)) = d(W(z_1'), W(z_2)) = d(z_1', z_2) < d(z_1, z_2)$.

(2) z_1 and z_2 are in different regions without a common boundary. We may apply the previous process to bring both z_1 and z_2 into the same region. □

4. Finite number of non similar generated triangles

In this section it will be proved that the iterative application of the longest-edge bisection to any initial triangle and its descendants only produce a finite number of distinct (up to similarity) triangles. This result will be shown by demonstrating that the orbit of any initial triangle is always finite. Before, however, we need the concepts of *closed set for bisection* and orbit of a point given by the following definitions.

Definition 4.1.
A region Ω is called a *closed region for LE–bisection* if for all $z \in \Omega$, then $w_L(z) \in \Omega$ and $w_R(z) \in \Omega$.

Of course, the normalized region is trivially a closed region for bisection.

Definition 4.2.
Let z in the normalized region. Let $\Gamma_z^{(0)} = \{z\}$ and $\Gamma_z^{(n+1)} = w_L\left(\Gamma_z^{(n)}\right) \cup w_R\left(\Gamma_z^{(n)}\right)$ for $n \geq 0$. The ***orbit*** of z is the set Γ_z defined by $\Gamma_z = \bigcup_{n\geq 0} \Gamma_z^{(n)}$.

For example if $\zeta = \frac{1}{2} + \frac{1}{2}i$, which corresponds to the right isosceles triangle, then $\Gamma_\zeta = \{\zeta\}$ since the longest-edge bisection of this triangle produces two triangles similar to the original one. Also if $v_0 = \frac{1}{2} + \frac{\sqrt{3}}{2}i$, which corresponds to the equilateral triangle, then $\Gamma_{v_0} = \{v_0, v_1, v_2\}$, where $v_1 = \frac{1}{4} + \frac{\sqrt{3}}{4}i$, and $v_2 = \frac{1}{2} + \frac{\sqrt{3}}{6}i$. See Figure 7.

Figure 7. Regions used in Lemmas in Section 4. All the lines in the set are geodesic lines of the Poincaré half-plane. Points $q_1 = \frac{3}{8} + \frac{\sqrt{23}}{8}i$ and $q_2 = \frac{5}{12} + \frac{\sqrt{23}}{12}i$ make an orbit with exactly two elements.

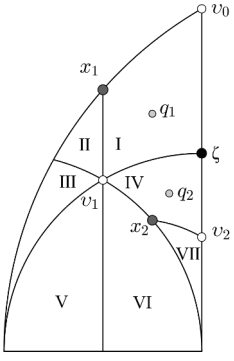

It follows from the definition, that the orbit of a point Γ_z is a closed region. However, outside the orbits there are other closed sets, as those given in the next Proposition.

Proposition 4.3.
Let z be a complex number in the normalized region Σ. Let Ω be the intersection with Σ of the union of the hyperbolic circles with centres in Γ_z and with the same radius r. Then Ω is a closed set for the LE-bisection.

Proof. Let ω be in Ω. By definition of orbit, there exists a z' in Γ_z such that $d(\omega, z') \leq r$. If W is any of the functions $w_L(z)$ and $w_R(z)$, by the non-increasing property of Lemma 3.2, then $d(W(\omega), W(z')) \leq r$. Hence, $W(\omega) \in \Omega$ because $W(z') \in \Gamma_z$. □

In the sequel below, we will prove in a straight way that for any point z in the union of regions *I*, *II* or *IV* its orbit is finite.

Lemma 4.4.
The union of the regions I and IV in the normalized region as labeled in Figure 7 is a closed region. In addition, for $z \in I \cup IV$ then the cardinal of its orbit, $|\Gamma_z|$, is finite.

Proof. It is enough to check the images of the corner points of regions *I* and *IV*. This is because the boundary lines of these regions are geodesic lines and functions $w_L(z)$ and $w_R(z)$ are isometries of the hyperbolic plane. For example,

$w_R(I) = IV$ since $w_R(\zeta) = \zeta$, $w_R(v_0) = v_1$, $w_R(x_1) = x_2$, and $w_R(v_1) = v_2$. In the same way it may be proved easily that $w_L(I) = I$, $w_L(IV) = I$, and $w_R(IV) = IV$. Therefore the union of I and IV is a closed region for LE-bisection.

Note that for $z \in I$, $w_L(z) = \frac{1}{2\bar{z}}$ which is an inversion with respect to the geodesic $|z| = \frac{\sqrt{2}}{2}$. On the other hand, for $z \in IV$, $w_R(z) = \frac{2\bar{z}-1}{2\bar{z}-2}$ which is an inversion with respect to the geodesic $|z-1| = \frac{\sqrt{3}}{2}$. Also, for $z \in I$, $w_R(z) = \frac{-1}{2z-2}$ which is a hyperbolic rotation of $\pi/2$ radians with center ζ. For $z \in IV$, $w_L(z) = \frac{2z-1}{2z}$ which is a hyperbolic rotation of $-\pi/2$ radians with center ζ. With these information, it is straightforwardly deduced that a typical orbit for a point $z \in I \cup IV$ is of the form $\Gamma_z = \left\{z, \frac{1}{2\bar{z}}, \frac{-1}{2z-2}, \frac{\bar{z}}{2\bar{z}-1}\right\}$, and consequently is finite. Figure 8 shows the elements of the orbit of a point $z \in I$. □

Figure 8. Closed graph describing the orbit of point $z \in I$.

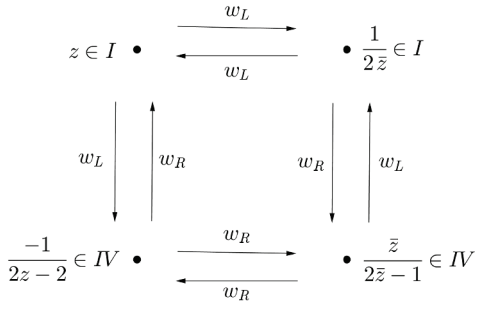

Remark 4.5.

It should be noted that an orbit may have less than four elements. In a tipical orbit may appear some coincidences that produce that the orbit presents a lower cardinal. An orbit of importance in the proof of the finiteness of the orbits for the longest-edge bisection and of exactly two elements is the set $\left\{q_1 = \frac{3}{8} + \frac{\sqrt{23}}{8}i, q_2 = \frac{5}{12} + \frac{\sqrt{23}}{12}i\right\}$. In fact, as it is easy to check $w_L(q_1) = q_1$, $w_R(q_1) = q_2$, $w_L(q_2) = q_1$, and $w_R(q_2) = q_2$. See Figure 7.

Lemma 4.6.

If $z \in II$ in the normalized region as labeled in Figure 7, then the cardinal of its orbit, $|\Gamma_z|$, is finite.

Proof. By the simmetry of function $w_L(z)$ with respect to the line Re $z = \frac{1}{4}$, then $w_L(z) = \frac{-1}{2z-1} \in I$. Besides, $w_R(z) = \frac{-1}{2z-2} \in VII$. Hence, $w_L(w_R(z)) = z$ and $w_R^2(z) = \frac{\bar{z}}{2\bar{z}-1} \in VI$. Also, $w_R^3(z) = w_R(z)$, and $w_L\left(w_R^2(z)\right) = w_L(z) \in I$. It follows that the cardinal of its orbit, $|\Gamma_z|$, is finite by Lemma 4.4. Figure 9 shows the elements of the orbit of a point $z \in II$. □

Figure 9. Closed graph describing the orbit of point $z \in II$. Out of region I are only z, $w_R(z)$ and $w_R^2(z)$.

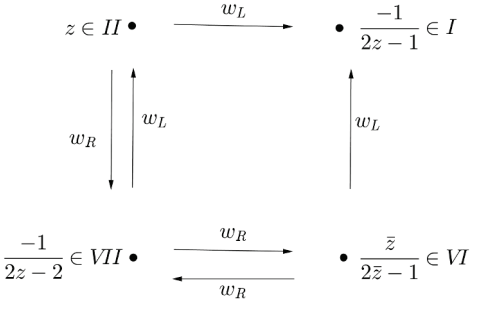

To employ that a similar argument to the previous one other regions seems long-winded. Instead, we will extend the result about finite orbits to a closed region given by hyperbolic circles with centers q_1 and q_2. We will prove first the property for the points in the orbit of equilateral triangle.

Lemma 4.7.

There exists $\epsilon' > 0$ such that for every z in the normalized region with hyperbolic distance less or equal than ϵ' to any of the points v_0, v_1 and v_2, the cardinal $|\Gamma_z| < \infty$.

Proof. Notice that ϵ' may be chosen such that every circle with centre v_i does not overlap a region not containing point v_i on its boundary. See Figure 10.

Figure 10. Number $\epsilon' > 0$ is chosen in such a way that each circle with center at v_0, v_1, or v_2, and radious ϵ' only overlaps the regions with boundary containing its center.

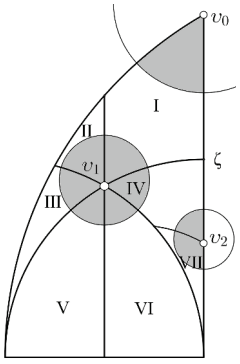

Let z in the normalized region with $d(z, v_0) \leq \epsilon'$. Then $z \in I$ and $|\Gamma_z| < \infty$.

If, otherwise, $d(z, v_1) \leq \epsilon'$, then $w_L(z) \in I$. In addition, by the simmetry of $w_R(z)$ with respect to $\left|z - \frac{1}{2}\right| = \frac{\sqrt{2}}{2}$ we may assume that $z \in IV \cup V \cup VI$. Therefore, $w_R(z) = \frac{2\bar{z}-1}{2\bar{z}-2} \in IV \cup VII$, and $w_R^2(z) = z$. Since function w_L in $IV \cup VII$ is a hyperbolic rotation of $-\frac{\pi}{2}$ radians with centre point ζ, then $w_L(w_R(z)) = \frac{\bar{z}}{2\bar{z}-1} \in I \cup II \cup III$. And then, $w_L^2(w_R(z)) \in I$. Also, $w_R(w_L(w_R(z))) = w_R(z)$ because function $w_L(z)$ for $z \in IV \cup VII$ is a hyperbolic rotation of $\frac{\pi}{2}$ radians with center at ζ. Since

$$\Gamma_z = \{z, w_R(z), w_L(w_R(z))\} \cup \Gamma_{w_L(z)} \cup \Gamma_{w_L^2(w_R(z))}$$

it follows that $|\Gamma_z| < \infty$ by Lemma 4.4.

If, finally, $d(z, v_2) \leq \epsilon'$, then $d(w_L(z), v_1) \leq \epsilon'$ and also $d(w_R(z), v_1) \leq \epsilon'$, so this case is reduced to the previous one. □

Lemma 4.8.

Let $q_1 = \frac{3}{8} + \frac{\sqrt{23}}{8}i$ and $r = d(q_1, v_1)$. Then, there exists $\epsilon > 0$ such that for any z in the normalized region with $d(q_1, z) \leq r + \epsilon$, the cardinal $|\Gamma_z| < \infty$.

Proof. Observe that ϵ may be chosen such that every circle with centre q_1 does not overlap region VII. See Figure 11. This is possible since $d(q_1, v_1) < d(q_1, x_2)$. For such ϵ, we can assure that the region $\{z$ such that $d(q_1, z) < r + \epsilon\}$ is contained in the set $I \cup II \cup IV$ together with a small hyperbolic circle with centre v_1 as in Lemma 4.7. □

Lemma 4.9.

Let $q_2 = \frac{5}{12} + \frac{\sqrt{23}}{12}i$ and r and ϵ as in Lemma 4.8. Then, for any z in the normalized region with $d(q_2, z) \leq r + \epsilon$, the cardinal $|\Gamma_z| < \infty$.

Figure 11. Number $\epsilon > 0$ is chosen now in such a way that every circle with centre q_1 does not overlap region VII. Circle with center at q_1 and radious $d(q_1, v_1) + \epsilon$ is included in the union of regions I, II and IV along with a small circle with center at v_1.

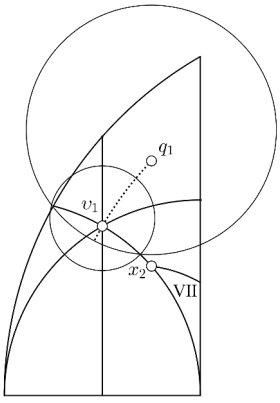

Proof. Note that $|z-1/2| = 1/2$ is the normal bisector of the segment q_1 y q_2. If $|z-1/2| \geq 1/2$ then $d(z, q_1) \leq r+\epsilon$ and Lemma 4.8 applies. We may assume that $|z-1/2| \leq 1/2$, and therefore that $z \in IV \cup V \cup VI \cup VII$. Therefore $w_R^2(z) = z$. Then

$$\Gamma_z = \{z, w_R(z)\} \cup \Gamma_{w_L(z)} \cup \Gamma_{w_L(w_R(z))}.$$

Since $d(w_L(z), q_1) \leq d(z, q_2) \leq r + \epsilon$, then $|\Gamma_{w_L(z)}| < \infty$. In the same way, also $|\Gamma_{w_L(w_R(z))}| < \infty$ since

$$d(w_L(w_R(z)), q_1) \leq d(w_R(z), q_2) \leq d(z, q_2) \leq r + \epsilon.$$

Because Γ_z is the union of finite sets, the result follows. □

Lemma 4.10.

Let ϵ be as in Lemma 4.8 and $r = d(q_1, v_1)$. Let K be a compact set into the normalized region such that if $z \in K$, then $r + \epsilon \leq d(z, q_1)$. Then, there exists a value A, with $0 < A < 1$ such that $d(w_L(z), q_1) \leq A \cdot d(z, q_1)$.

Proof. Function $\varphi(z) = \frac{d(w_L(z), q_1)}{d(z, q_1)}$ is continuous on K. In addition, if $z \in K$, then $z \notin I$. So, by the non-increasing property, $d(w_L(z), q_1) < d(z, q_1)$ since $w_L(q_1) = q_1$. Therefore, $\varphi(z) < 1$, for $z \in K$. In particular this hold for the maximum of $\varphi(z)$, $A < 1$. □

Theorem 4.11 (Finite orbits).

Let z be in the normalized region. Then $|\Gamma_z| < \infty$.

Proof. Let r and ϵ as in Lemma 4.8. If $d(z, q_1) \leq r + \epsilon$, then $|\Gamma_z| < \infty$ by Lemma 4.8. Also, if $d(z, q_2) \leq r + \epsilon$, then $|\Gamma_z| < \infty$ by Lemma 4.9. We may assume that $d(z, q_1) > r + \epsilon$ and $d(z, q_2) > r + \epsilon$. In this situation, as it is shown in Figure 12 the orbit of point z given by

$$\Gamma_z = \{z, w_R(z), w_R^2(z)\} \cup \Gamma_{w_L(z)} \cup \Gamma_{w_L(w_R(z))} \cup \Gamma_{w_L(w_R^2(z))}.$$

Let K the compact set comprised by the points u in the normalized region such that $d(u, q_1) \leq d(z, q_1)$ or $d(u, q_2) \leq d(z, q_2)$, and at the same time $d(u, q_1) \geq r + \epsilon$ and $d(u, q_2) \geq r + \epsilon$. See Figure 13.

Figure 12. The orbit of any point z may be written as $\Gamma_z = \{z, w_R(z), w_R^2(z)\} \cup \Gamma_{w_L(z)} \cup \Gamma_{w_L(w_R(z))} \cup \Gamma_{w_L(w_R^2(z))}$.

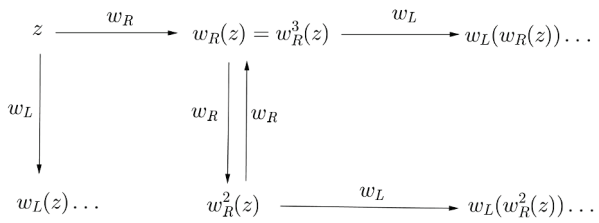

Figure 13. Compact set K such that for $u \in K$, $d(u, q_1) \leq d(z, q_1)$ or $d(u, q_2) \leq d(z, q_2)$, and at the same time $r + \epsilon \leq d(u, q_1)$ and $r + \epsilon \leq d(u, q_2)$.

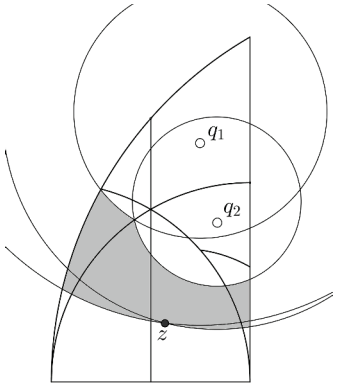

By Lemma 4.10, there exists a constant A such that for any $u \in K$, there is $d(w_L(u), q_1) \leq A \cdot d(u, q_1)$. Therefore, $d(w_L(z), q_1) \leq A \cdot d(z, q_1)$. Besides, by the non-increasing property $d(w_R(z), q_2) \leq d(z, q_2)$. Then, either $w_R(z) \in K$ and $d(w_L(w_R(z)), q_1) \leq A \cdot d(w_R(z), q_1)$, or the orbit of $w_R(z)$ is finite, and also in particular is finite the orbit of $w_L(w_R(z))$.

Since, also by the non-increasing property, we have that $d(w_R^2(z)), q_2) \leq d(w_R(z), q_2) \leq d(z, q_2)$ it follows that either $d(w_L(w_R^2(z)), q_1) \leq A \cdot d(w_R^2(z), q_1)$, or the orbit of $w_L(w_R^2(z))$ is finite, and also in particular is finite the orbit of $w_L(w_R^2(z))$.

In conclusion, the orbit of point z is described as union of a finite set of points, say B, and a finite number of orbits either finite or of points closer to q_1 than the points of the set B. We may iterate the same process as many times as necessary to finally describe the orbit Γ_z as a finite set and a finite number of orbits, either finite or orbits of points with distance to q_1 less or equal than $r + \epsilon$. Therefore, by Lemma 4.8 these orbits also are finite. □

5. Non-degeneracy property of the longest-edge bisection

The non-degeneracy of the longest-edge bisection follows from the fact that only finite number of similar triangles are generated. This already shows that the minimum angle does not tend to zero. Further we give a lower bound for the minimum angle, also using concepts from hyperbolic geometry in the normalized region. Although the result is well-known [23, 24], the approach used here is new and could be applied for the other longest-edge partition methods.

Theorem 5.1 (Lower bound on the angles of triangles constructed by LE- bisection).
Let α be the smallest angle of an initial triangle. Let α' be the minimum interior angle in new triangles generate the iterative LE–bisection of the initial triangle. Then $\alpha' \geq \alpha/2$.

We will cover the normalized region with subsets in which the statement of the theorem holds. The first subset, Ω is determined by four points: the fixed point for the LE-bisection, $\zeta = \frac{1}{2} + \frac{1}{2}i$, and the three points of the orbit of the equilateral triangle. See Figure 14. Let D be the hyperbolic semicircle with centre ζ and tangent to the line Re $z = \frac{1}{4}$. By the non-increasing property, D is a closed region of the LE-bisection. The hyperbolic radius of D is ln $\left(\frac{1+\sqrt{5}}{2}\right)$.

Figure 14. Orbit of the equilateral triangle (white points), orbit of the isosceles right triangle (black point), semicircle D, and region Ω in grey.

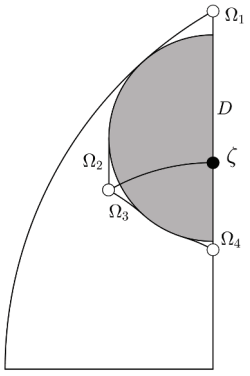

Let Ω_1 the region between the circumference $|z-1| = 1$, the boundary of D and the line Re $z = \frac{1}{2}$. Let Ω_2 the region between the circumference $\left|z - \frac{1}{2}\right| = \frac{1}{2}$, the boundary of D and the line Re $z = \frac{1}{4}$. Let Ω_3 the region between the circumferences $\left|z - \frac{1}{2}\right| = \frac{1}{2}$ and $|z| = 1/2$, and the boundary of D. Finally, let Ω_4 the boundary of D, the line Re $z = \frac{1}{2}$ and the geodesic hyperbolic tangent to the boundary of D passing through point $\frac{1}{2} + \frac{\sqrt{3}}{6}i$. Then,

$$w_L(\Omega_1) = \Omega_2,\ w_R(\Omega_1) = \Omega_3,\ w_L(\Omega_2) = \Omega_1,\ w_R(\Omega_2) = \Omega_4$$
$$w_L(\Omega_3) = \Omega_1,\ w_R(\Omega_3) = \Omega_4,\ w_L(\Omega_4) = \Omega_2,\ w_R(\Omega_4) = \Omega_3.$$

Therefore, region $\Omega = D \cup \Omega_1 \cup \Omega_2 \cup \Omega_3 \cup \Omega_4$ is a closed region for the LE-bisection.

Proposition 5.2.
Let $z \in \Omega$ and z' in the orbit Γ_z. Let α and α' respectively be the arguments of complex numbers $1-\overline{z}$ and $1-\overline{z'}$. Then $\alpha' \geq \alpha/2$.

Proof. The tangent line to the boundary of D through point $1 = 1 + 0i$ intersects the boundary of D at point $w = \frac{10-\sqrt{10}}{18} + \frac{2\sqrt{5}-\sqrt{2}}{8}i$, and it is between Ω_3 and Ω_4. Let $\theta = \text{Arg}(1-\overline{w})$. Then $\tan\theta = \frac{2(\sqrt{5}-\sqrt{2})}{3}$ and $\tan(2\theta) = \frac{4(7\sqrt{2}+\sqrt{5})}{31}$. See Figure 15.

For the point $\frac{1}{3} + \frac{\sqrt{5}}{3}i$, the tangent of the angle between the straight line passing through $1 = 1 + 0\cdot i$ and the negative real axis is $\frac{\sqrt{5}}{2} < \tan(2\theta)$. Therefore, for every z below the straight line passing through $1 = 1 + 0\cdot i$ and $\frac{1}{3} + \frac{\sqrt{5}}{3}i$, the proposition follows.

We proceed now to prove the proposition for the points on the normalized region over the straight line with angle arctan $\left(\frac{\sqrt{5}}{2}\right)$. The composition of functions w_L and w_R producing the worst case is such that the point $\frac{1}{2} + \frac{\sqrt{3}}{2}i$ is transformed in $\frac{1}{2} + \frac{\sqrt{3}}{6}i$, point $\frac{1}{3} + \frac{\sqrt{5}}{3}i$ is sent to $\frac{3}{7} + \frac{\sqrt{5}}{7}i$, while point $\frac{1}{2} + \frac{1}{2}i$ is invariant. So, it is and inversion, say T, with respect to the circumference $|z - 1/2| = 1/2$.

Let ξ be a point on the circular arc $|z-1| = 1$ between points $\frac{1}{2} + \frac{\sqrt{3}}{2}i$ and $\frac{1}{3} + \frac{\sqrt{5}}{3}i$. Let ξ' be the image of ξ by inversion T: $T(\xi) = \xi'$. See Figure 16. Point ξ' is located on the tangent geodesic to the boundary of D passing through point $\frac{1}{2} + \frac{\sqrt{3}}{6}i$. The half line joining point $1 + 0\cdot i$ and ξ is an equidistant curve from the geodesic line Re $z = 1$. Its image by T is the equidistant curve to the geodesic $|z - 3/4| = 1/4$. This equidistant curve passes through points $\frac{1}{2}$, ξ' and 1. For

Figure 15. Proving the lower bound on the angles in region Ω.

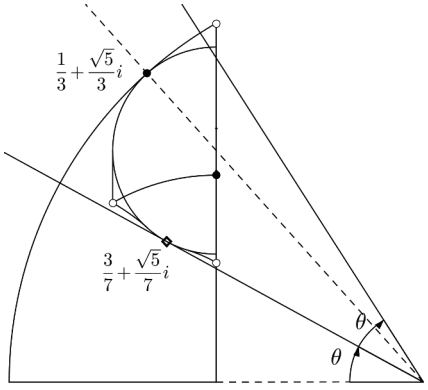

Figure 16. Point ξ is the highest one on the ray and point ξ' is its image on the semicircumference.

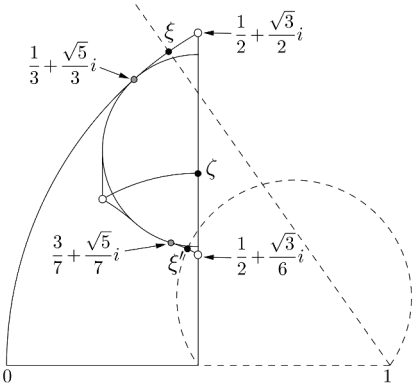

the points of the straight line between $1+0\cdot i$ and ξ into the normalized region, the highest quotient α/α' is obtained for ξ and it image, ξ', which are the highest and the lowest points in both equidistant lines.

The limit case holds for $\xi = \frac{1}{2}+\frac{\sqrt{3}}{2}i$ and $\xi' = \frac{1}{2}+\frac{\sqrt{3}}{6}i$ and the quotient is $\alpha/\alpha' = 2$. □

Now we have to consider the non-degeneracy question for the points below the boundary of D.

Proposition 5.3.
Let z be in the normalized region below the boundary of D and z' in the orbit Γ_z. Let α and α' respectively be the arguments of complex numbers $1-\overline{z}$ and $1-\overline{z'}$. Then $\alpha' \geq \alpha/2$.

Proof. For any point z in the region under consideration, we may consider the hyperbolic circumference with centre $\zeta = \frac{1}{2}+\frac{1}{2}i$ passing through z, with radius $r' \geq r = \ln\left(\frac{1+\sqrt{5}}{2}\right)$. Let ξ be the intersection point of the previous circumference with the circumferece $|z-1| = 1$ as in Figure 17.

Let ξ' be point of the tangent line to the circumference from the point $1 = 1+0\cdot i$. By the non-increasing property, any point of the orbit of z is inside the circumference with centre $\zeta = \frac{1}{2}+\frac{1}{2}i$ passing through z. Therefore, the arguments of $1-\overline{\xi}$ and $1-\overline{\xi'}$ give an upper bound of α/α'. See Figure 17.

We have that by Equation (3)

$$\frac{\alpha}{\alpha'} \leq \frac{\arctan\left(e^{-x-r_0}\right)}{\arctan\left(e^{-r'-r'_0}\right)}.$$

Figure 17. Values used in the proof of Proposition 5.3.

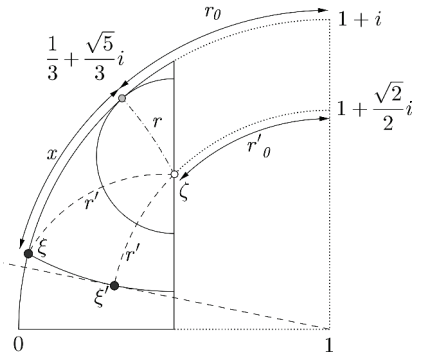

Since $\arctan\delta \le \delta$ for $\delta \ge 0$, then $\arctan(e^{-x-r_0}) \le e^{-x-r_0}$. In addition, by Equation (3)

$$e^{-r'-r'_0} \le \tan\left(\frac{\theta}{2}\right), \text{ with } \tan\theta = \frac{2(\sqrt{5}-\sqrt{2})}{3}.$$

For $0 \le \delta \le \tan\left(\frac{\theta}{2}\right)$ it holds that

$$m\delta \le \arctan\delta, \text{ where } m = \frac{\theta/2}{\tan(\theta/2)}.$$

Therefore,

$$\frac{\alpha}{\alpha'} \le \frac{1}{m} e^{(r'-x)+(r'_0-r_0)}.$$

By the hyperbolic version for the Pythagorean Theorem $\cosh x \cdot \cosh r = \cosh r'$. Since $r = \ln\left(\frac{1+\sqrt{5}}{2}\right)$, then $\cosh x = \frac{2}{\sqrt{5}}\cosh r'$. And therefore,

$$e^{r'-x} = \frac{e^{r'}}{e^x} = \frac{e^{r'}}{\frac{2}{\sqrt{5}}\cosh r' + \sqrt{\frac{4}{5}\cosh^2 r' - 1}} \le \frac{e^{r'}}{\frac{4}{\sqrt{5}}\cosh r' - 1} = \frac{e^{r'}\sqrt{5}}{4\cosh r' - \sqrt{5}}.$$

The maximum value of the previous expression is attained for $r' = \ln\left(\frac{4}{\sqrt{5}}\right)$, then $e^{r'-x} \le \frac{8\sqrt{5}}{11}$.

By the formula for the hyperbolic distance, $\cosh r_0 = \frac{3}{\sqrt{5}}$ and $\cosh r'_0 = \sqrt{2}$, and so, $e^{r_0} = \sqrt{5}$ and $e^{r'_0} = 1+\sqrt{2}$, from where $e^{r'_0-r_0} = \frac{1+\sqrt{2}}{\sqrt{5}}$. Finally,

$$\frac{\alpha}{\alpha'} \le \frac{1}{m} \cdot \frac{8\sqrt{5}}{11} \cdot \frac{1+\sqrt{2}}{\sqrt{5}} \approx 1.7935,$$

and the proof is complete. □

Proof of Theorem 5.1. Let z the complex number associated to the initial triangle. The triangles generated by iteration of LE–bisection from the initial triangle are associated with complex numbers z' in the orbit Γ_z. As the normalized region is covered by the two regions described in Propositions 5.2 and 5.3, in any case $\alpha' \ge \alpha/2$, where α and α' are the arguments of complex numbers $1-\overline{z}$ and $1-\overline{z'}$, respectively. Also α and α' are the minimum angles of the initial and any generated triangle, and the proof is completed. □

6. Conclusions

In this paper we have used concepts from hyperbolic geometry to prove two relevant properties of the longest-edge bisection of triangles. These properties are commonly required e.g. for the finite element method [2, 6, 14]. We have proved that the number of distinct (up to similarity) triangles generated by iterative application of the longest-edge bisection to any initial triangle is finite. Besides, and also by hyperbolic geometry, we have proved easily that the longest edge partition does not degenerate. More precisely, if α_0 is the minimum angle of an initial given triangle, and α is the minimum interior angle in new triangles considered after any number of iterations of longest-edge bisection, then $\alpha \geq \alpha_0/2$.

Acknowledgements

The authors would like to thank the anonymous referees for their helpful comments. This work has been supported in part by the CICYT Project number MTM2008-05866-C03-02/MTM from the Spanish Ministerio de Educación y Ciencia.

References

[1] Adler A., On the bisection method for triangles, Math. Comp., 1983, 40, 571–574
[2] Babuška I., Aziz A. K., On the angle condition in the finite element method. SIAM J. Numer. Anal. 1976, 13, 214–226
[3] Bern M., Eppstein D., Optimal Möbius transformations for information visualization and meshing, Lecture Notes in Comp. Sci., 2001, 2125, 14–25
[4] Bookstein F.L., Morphometric Tools for Landmark Data: Geometry and Biology, Cambridge University Press, 1991
[5] Brandts J., Korotov S., Křížek M., On the equivalence of regularity criteria for triangular and tetrahedral finite element partitions, Comput. & Math. Appl., 2008, 55, 2227–2233
[6] Ciarlet P. G., The Finite Element Method for Elliptic Problems. North-Holland, Amsterdam, 1978.
[7] Dryden I.L., Mardia K.V., Statistical Shape Analysis, Wiley, 1998
[8] Eppstein D., Manhattan orbifolds, Topology and its Applications, 2009,157(2), 494–507
[9] Eppstein D., Succinct greedy geometric routing using hyperbolic geometry, IEEE Transactions on Computing, 2011, 60(11), 1571–1580
[10] Gutiérrez C., Gutiérrez F., Rivara M.-C., Complexity of bisection method, Theor. Comp. Sci., 2007, 382, 131–138
[11] Hannukainen A., Korotov S., Křížek M., On global and local mesh refinements by a generalized conforming bisection algorithm, J. Comput. Appl. Math., 2010, 235, 419–436
[12] Iversen B., Hyperbolic Geometry, Cambridge University Press, 1992
[13] Korotov S., Křížek M., Kropác A., Strong regularity of a family of face-to-face partitions generated by the longest-edge bisection algorithm, Comput. Math. and Math. Phys., 2008, 49, 1687–1698
[14] Křížek M., On semiregular families of triangulations and linear interpolation, Appl. Math., 1991, 36, 223–232
[15] Márquez A., Moreno-González A., Plaza A., Suárez J. P., The seven-triangle longest-side partition of triangles and mesh quality improvement, Finite Elem. Anal. Des., 2008, 44, 748–758
[16] Padrón M. A., Suárez J. P., Plaza A., A comparative study between some bisection based partitions in 3D, Appl. Num. Math., 2005, 55, 357–367
[17] Perdomo F., Plaza A., A new proof of the degeneracy property of the longest-edge n-section refinement scheme for triangular meshes, Appl. Math. & Compt., 2012, 219, 2342–2344
[18] Perdomo F., Plaza A., Proving the non-degeneracy of the longest-edge trisection by a space of triangular shapes with hyperbolic metric, Appl. Math. & Compt., 2013, 221, 424—432
[19] Perdomo F., Dynamics of the longest-edge partitions in a triangle space endowed with an hyperbolic metric, Ph.D. Thesis (in Spanish), Las Palmas de Gran Canaria, 2013

[20] Plaza A., Padrón M. A., Suárez J. P., Non-degeneracy study of the 8-tetrahedra longest-edge partition, Appl. Num. Math., 2005, 55, 458–472
[21] Plaza A., Suárez J. P., Padrón M. A, Falcón S., Amieiro D., Mesh quality improvement and other properties in the four-triangles longest-edge partition. Comp. Aid. Geom. Des., 2004, 21, 353–369
[22] Plaza A., Suárez J. P., Carey G. F., A geometric diagram and hybrid scheme for triangle subdivision, Comp. Aid. Geom. Des., 2007, 24, 19–27
[23] Rivara M.-C., Mesh refinement processes based on the generalized bisection of simplices, SIAM J. Num. Anal., 1984, 21, 604–613
[24] Rosenberg I. G., Stenger F., A lower bound on the angles of triangles constructed by bisecting the longest side, Math. Comp., 1975, 29, 390–395
[25] Stahl S., The Poincaré Half-Plane, Jones & Bartlett Learning, 1993
[26] Stynes M., On faster convergence of the bisection method for certain triangles, Math. Comp., 1979, 33, 717–721
[27] Stynes M., On faster convergence of the bisection method for all triangles, Math. Comp., 1980, 35, 1195–1201
[28] Toth G., Glimpses of Algebra and Geometry, Springer, 2002